ARTICLE

Check for updates

Epigenetic induction of lipocalin 2 expression drives acquired resistance to 5-fluorouracil in colorectal cancer through integrin β3/SRC pathway

Wenyi Zhang[1,2], Rulu Pan[1], Mei Lu[1], Qian Zhang[1], Ziqi Lin[1], Yuan Qin[1], Zhanyu Wang[1], Siqing Gong[1], Huan Lin[1], Shuyi Chong[1], Liting Lu[1], Wanqin Liao[3] and Xincheng Lu[1]✉

The therapeutic efficacy of 5-fluorouracil (5-FU) is often reduced by the development of drug resistance. We observed significant upregulation of lipocalin 2 (LCN2) expression in a newly established 5-FU-resistant colorectal cancer (CRC) cell line. In this study, we demonstrated that 5-FU-treated CRC cells developed resistance through LCN2 upregulation caused by LCN2 promoter demethylation and that feedback between LCN2 and NF-κB further amplified LCN2 expression. High LCN2 expression was associated with poor prognosis in CRC patients. LCN2 attenuated the cytotoxicity of 5-FU by activating the SRC/AKT/ERK-mediated antiapoptotic program. Mechanistically, the LCN2-integrin β3 interaction enhanced integrin β3 stability, thus recruiting SRC to the cytomembrane for autoactivation, leading to downstream AKT/ERK cascade activation. Targeting LCN2 or SRC compromised the growth of CRC cells with LCN2-induced 5-FU resistance. Our findings demonstrate a novel mechanism of acquired resistance to 5-FU, suggesting that LCN2 can be used as a biomarker and/or therapeutic target for advanced CRC.

Oncogene; https://doi.org/10.1038/s41388-021-02029-4

INTRODUCTION

Colorectal cancer (CRC) is one of the most common malignancies and the second leading cause of cancer-related death worldwide [1]. Drug resistance and metastasis contribute substantially to the poor prognosis of CRC patients. 5-Fluorouracil (5-FU) is a first-line chemotherapeutic agent used for the treatment of CRC. However, the therapeutic efficacy of 5-FU in CRC patients is frequently impeded by the low response rate and the development of drug resistance [2]. Identifying key markers and improving the understanding of the mechanisms underlying 5-FU resistance in CRC may improve its therapeutic effect.

5-FU exerts its anticancer effects by disrupting the action of thymidylate synthase (TYMS), thereby damaging RNA and DNA [3]. Multiple mechanisms, including disruption of 5-FU-metabolizing enzymes, changes in drug influx and efflux, and alteration of cellular processes, have been shown to play important roles in 5-FU resistance in CRC [4]. High expression levels of TYMS and increased activity of dihydropyrimidine dehydrogenase, both of which disrupt 5-FU metabolism, are widely accepted as the major molecular mechanisms responsible for 5-FU resistance [5, 6]. Expression of ATP-binding cassette (ABC) transporters, such as ABCB1 and ABCB5, is substantially increased in clinical CRC cases after 5-FU-based chemotherapy and contributes to the development of 5-FU resistance via efflux of anticancer agents from cancer cells [7, 8]. Evasion of apoptosis is another important cause of 5-FU resistance. Increased expression of antiapoptotic genes, such as Bcl-2 and Bcl-xl, as well as decreased expression of the proapoptotic gene p53 and Bax, has been shown to be correlated with 5-FU resistance in CRC [9–11]. In addition, activation of autophagy and epithelial-mesenchymal transition (EMT) has been described to mediate 5-FU resistance in CRC [12, 13]. Although multiple factors have been reported to contribute to 5-FU resistance, the mechanisms of acquired resistance to 5-FU are incompletely elucidated. Moreover, most of the reported mechanisms are limited to explaining the causes of 5-FU resistance and hardly explain acquired 5-FU resistance.

Aiming to screen potential driver genes of acquired 5-FU resistance in CRC, we established CRC cell lines with acquired 5-FU-resistance and then performed an in vitro transcriptome sequencing analysis. We found that the expression of lipocalin 2 (LCN2) was highly upregulated in CRC cell lines with acquired 5-FU-resistance. LCN2, also called neutrophil gelatinase-associated lipocalin (NGAL), is a secreted glycoprotein that was first identified as an essential component of the antimicrobial innate immune system [14]. It attenuates bacterial growth by preventing bacterial iron acquisition [15]. LCN2 can bind to and transport small lipophilic molecules, such as steroid hormones, lipids, and retinoids [16], and its dysregulation has been linked to cardiovascular diseases, obesity, and metabolic syndrome [17, 18]. LCN2 is also an established biomarker for renal injury, and the LCN2 level is increased in the serum of patients with psoriasis [19, 20]. LCN2 is expressed at a high level in various tumors and can facilitate tumorigenesis by promoting survival, growth, and metastasis [21–24]. In CRC, an increased LCN2 expression level is correlated with tumorigenesis and poor prognosis [25]. Recent

[1]School of Basic Medical Sciences, Wenzhou Medical University, Wenzhou 325035, China. [2]Department of Radiotherapy, The First Affiliated Hospital of Wenzhou Medical University, Wenzhou, China. [3]Department of Basic Medicine and Biomedical Engineering, Foshan University, Foshan 528200, China. ✉email: xinchenglu@yahoo.com

Received: 18 March 2021 Revised: 3 September 2021 Accepted: 17 September 2021
Published online: 29 September 2021

studies have reported that alterations in LCN2 expression are associated with sensitivity to certain anticancer drugs. However, the role of LCN2 in drug chemosensitivity is controversial. For example, downregulation of LCN2 induces vincristine resistance in CRC [26], whereas overexpression of LCN2 reduces the cytotoxity of gemcitabine [27] and TNF-related apoptosis-inducing ligand (TRAIL) [28] in pancreatic and colon cancer, respectively. In oral cancer, LCN2 is associated with vitamin D-promoted cisplatin chemosensitivity [29]. These studies suggest that the role of LCN2 on chemosensitivity may differ depending on the cancer type and its exact mechanism of action in drug resistance remains largely unknown. Until now, no attempt was made to examine the role of LCN2 on acquired 5-FU resistance in CRC.

In this study, we investigated the function of LCN2 in acquired 5-FU resistance. We showed that LCN2 expression was significantly upregulated in 5-FU-resistant CRC cells and that LCN2 upregulation was associated with poor prognosis in CRC patients. LCN2 drove acquired 5-FU resistance both in vitro and in a xenograft model. Mechanistically, epigenetic induction of LCN2 activated a LCN2/NF-κB positive feedback loop, which further amplified LCN2 expression, thus triggering integrin/SRC-mediated aberrant activation of the AKT/ERK pathway.

RESULTS

LCN2 is upregulated in CRC cells with acquired 5-FU-resistance

To screen potential 5-FU resistance driver genes, we generated 5-FU-resistant CRC cell lines, named as HT29R, HT29R1, and HT29R2, by long-term culture of HT29 cells in a medium containing 5-FU. As shown in Fig. 1A, 5-FU-resistant HT29 clones were about eightfold more resistant to 5-FU than the parental HT29 cells, and 5-FU significantly inhibited the clonogenic ability of HT29 cells but had little effect on three 5-FU-resistant HT29 cell lines (Fig. 1B). Accordingly, compared with HT29 cells, 5-FU-resistant HT29R cells exhibited markedly enhanced apoptosis resistance in response to 5-FU exposure (Fig. 1C, D). Next, we performed RNA expression profiling of 5-FU-resistant and parental HT29 cells. Analysis of the sequencing data identified 599 and 635 genes (>2-fold; FDR adjusted $P < 0.001$) that were induced and repressed, respectively, in HT29R cells. LCN2 was among the most upregulated genes in all three 5-FU-resistant HT29 cells compared with parental HT29 cells in the transcriptome dataset (Fig. 1E, F). Upregulation of LCN2 mRNA and protein expression was validated in 5-FU-resistant HT29 clones by qRT-PCR and western blotting, respectively (Fig. 1G).

To investigate the clinical relevance of LCN2 expression in CRC, we evaluated LCN2 protein expression by IHC using tissue microarrays containing primary tissues from 83 CRC patients who have received 5-FU based regimen as adjuvant therapy. The LCN2 protein level was markedly elevated in tumors with liver metastasis (Fig. 2A, B). High LCN2 protein levels were positively associated with liver metastasis, recurrence, and low overall survival (OS) rates in this CRC cohort (Fig. 2C, D). Consistent with the results in our CRC cohort, the mRNA expression level of LCN2 in metastatic liver tissues was significantly higher than that in normal liver tissues in another GEO microarray cohort (Fig. 2E). Furthermore, ELISA test showed that the serum level of LCN2 in patients with recurrent CRC after 5-FU treatment was higher than that in patients without recurrence (Fig. 2F). The detection of serum LCN2 level in a group of ten patients pre and post recurrence also found that the level of LCN2 increased after recurrence (Fig. 2G). Considered collectively, the strong correlations between elevated LCN2 expression and metastasis/recurrence of CRC suggest that LCN2 is an indicator of chemoresistance and poor prognosis in clinical patients.

LCN2 enhances the resistance of CRC cells to 5-FU

Next, we examined whether LCN2 can drive resistance to 5-FU in CRC. Cell growth assays demonstrated that knockdown of LCN2 in HT29R cells markedly resensitized them to 5-FU, while knockdown of the other two highly expressed genes DMKN or EPHB2 had no significant effect on the sensitivity of HT29R cells to 5-FU (Fig. 3A–C, Supplementary Fig. S1). Furthermore, silencing LCN2 in SW480 cells (with high LCN2 expression) enhanced their 5-FU chemosensitivity, whereas overexpression of LCN2 in RKO cells (with low LCN2 expression and was high sensitive to 5-FU treatment) induced resistance to 5-FU (Fig. 3D; Supplementary Fig. S2A–C). In addition, blocking the LCN2 protein with a monoclonal antibody against LCN2 in HT29R cells resensitized them to 5-FU (Fig. 3E). These results indicate that LCN2 mediates 5-FU sensitivity and resistance in CRC cells. To confirm that LCN2 is a driver of acquired 5-FU resistance in vivo, we inoculated shNC- (a nontargeted vector) or shLCN2-transduced HT29R cells subcutaneously into nude mice. Mice were intraperitoneally injected with 50 mg/kg doses of 5-FU every other day for a total of seven times, and tumor growth was measured once daily. The tumor volume and weight data showed that LCN2 depletion significantly inhibited the growth of 5-FU-resistant CRC tumors (Fig. 3F, G; Supplementary Fig. S2D). Taken together, these results indicate that LCN2 can induce 5-FU resistance in both cells and xenografts, supporting that LCN2 is a new driver and/or target of acquired 5-FU resistance in CRC.

LCN2 induces 5-FU resistance by activating SRC/AKT/ERK cascades

We next sought to determine the mechanism responsible for LCN2-induced 5-FU resistance in CRC. Gene set enrichment analysis and Kyoto Encyclopedia of Genes and Genomes (KEGG) pathway (gene ontology) analysis showed that RAS/MAPK pathways were markedly enriched in upregulated genes in HT29R cells (Fig. 4A; Supplementary Fig. S3A). Western blot analysis showed that the activity of RAS and the levels of phosphorylated RAF/MEK/ERK, phosphorylated AKT, and its effector S6 were significantly elevated in HT29R cells compared with HT29 cells, while the phosphorylation of JNK and p38 were not significantly changed (Fig. 4B; Supplementary Fig. S3B–D). Furthermore, shRNA knockdown of LCN2 in HT29R and SW480 cells demonstrated a selective inhibition of AKT, as well as ERK, phosphorylation (Fig. 4C). In contrast, overexpression of LCN2 promoted the phosphorylation of both AKT and ERK in RKO cells (Supplementary Fig. S3E). In addition, suppression of the aberrant activation of these pathways by treatment with PI3K inhibitors (LY29004 and GDC0941) or an MEK/ERK inhibitors (U0126 and Trametinib) enhanced apoptosis and partially restored the sensitivity of HT29R cells to 5-FU (Supplementary Fig. S4). Collectively, these results suggest that LCN2-mediated activation of the antiapoptotic AKT/ERK pathway drives 5-FU resistance in CRC. Next, we examined the mechanism by which LCN2 induces AKT/ERK activation. Western blot analysis of the upstream pathways demonstrated that the phosphorylated SRC (Tyr416) level was significantly elevated in HT29R cells compared with HT29 cells, while the levels of p-SRC (Tyr527) and PTEN were not changed (Fig. 4D). Furthermore, depletion of LCN2 in HT29R and SW480 cells, by shRNA transfection decreased the p-SRC (Tyr416) level, whereas overexpression of LCN2 in RKO cells increased the p-SRC (Tyr416) level (Fig. 4E; Supplementary Fig. S5A). These data indicated that the activation (Tyr416 phosphorylation) of SRC in CRC cells was driven by LCN2 overexpression. Treatment with the SRC inhibitors eCF506 or saracatinib not only suppressed AKT/ERK signaling pathway activation in a dose-dependent manner but also abrogated the resistance of HT29R cells to 5-FU, as observed in both MTT and clonogenic assays (Fig. 4F; Supplementary Fig. S5B–F). Moreover, the combination of 5-FU with saracatinib was obviously superior to either monotherapy in inhibiting the growth of HT29R cells in nude mice, and the addition of saracatinib greatly weakened the resistance of HT29R cells to 5-FU (Fig. 4G, H). Collectively, these results suggest that blocking SRC activation can overcome

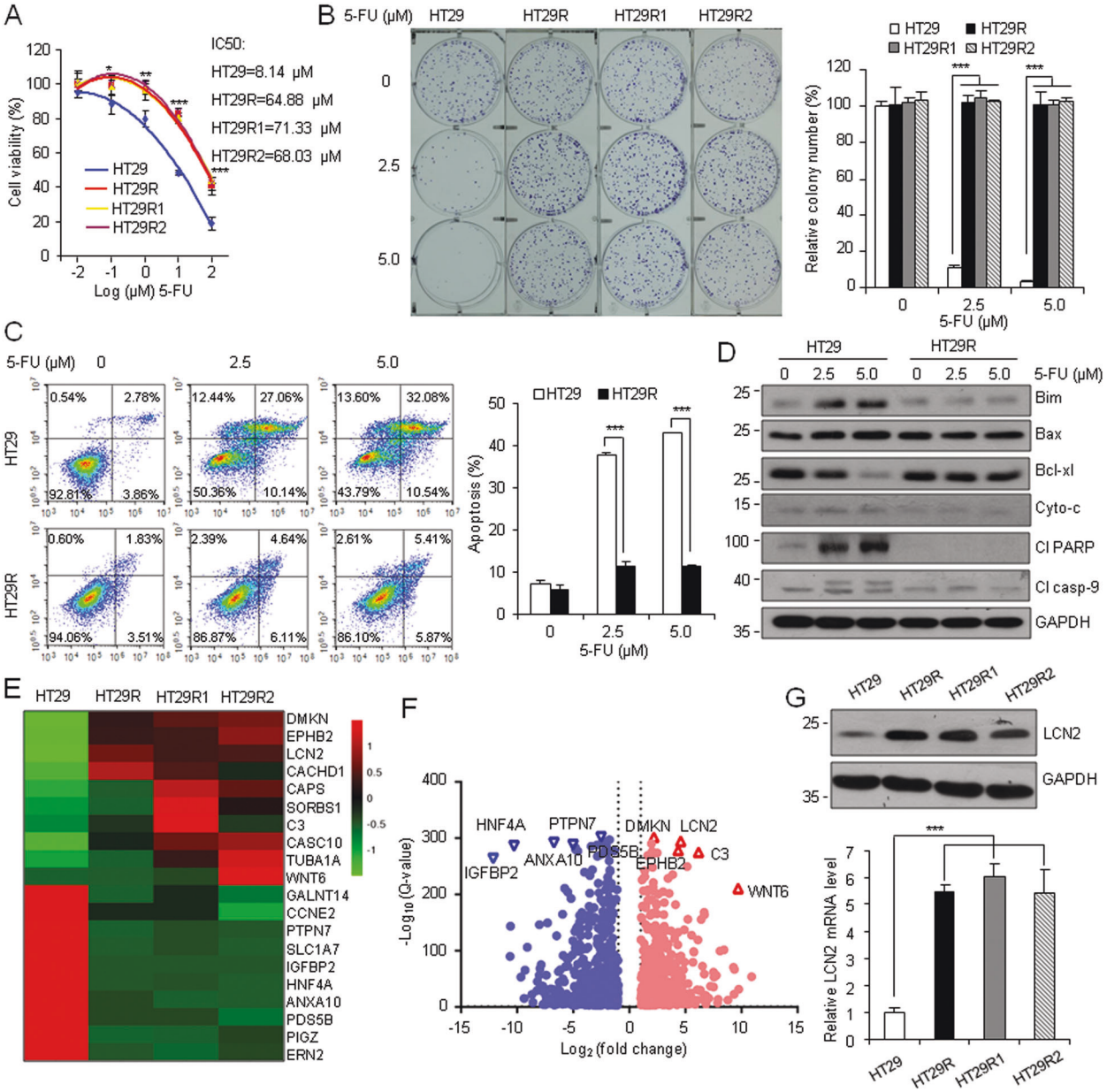

Fig. 1 LCN2 is upregulated in 5-FU-resistant CRC cells. A HT29 cells were treated with 0.01–2 μg/ml of 5-FU for months to generate 5-FU-resistant HT29 cells. The viability of parental HT29 and three 5-FU-resistant HT29 cell lines (HT29R, HT29R1, and HT29R2) was examined by MTT assay. Cells were treated with 5-FU (0.01–100 μM) for 72 h. The IC50 was defined as the concentration of 5-FU resulting in a 50% reduction in the number of cells compared with the number of untreated control cells. **B** Cell growth was determined by a clonogenic assay. Cells were incubated with control, 2.5 μM 5-FU or 5.0 μM 5-FU for 48 h and allowed to form colonies for 14 days. Left panel, representative images of the assay. **C** The apoptosis resistance capability of HT29R cells was analyzed by flow cytometry. Cells were incubated with control (DMSO), 2.5 μM or 5.0 μM 5-FU for 72 h. Left panel, representative images of the apoptosis assay are shown. Right panel, the numbers of apoptotic cells (%, Q2 + Q4) were calculated and are shown as the mean ± SD values. **D** The levels of apoptosis-related proteins in HT29 and HT29R cells were analyzed by western blot. HT29 and HT29R cells were incubated with control, 2.5 μM 5-FU or 5.0 μM 5-FU for 72 h. Cl PARP, cleaved PARP. Cl Casp-3, cleaved caspase-3. **E** Heatmap showing differentially expressed genes between HT29 and three 5-FU-resistant HT29 cells. **F** Volcano plot showing differentially expressed genes between HT29 and HT29R cells **G** Elevated LCN2 expression in 5-FU-resistant HT29 cells was validated by qRT-PCR and western blot analysis, respectively. In **A**, **B**, **C** and **G** data are shown as the mean ± SD values. The error bars indicate the SD of three independent experiments. *$P < 0.05$, **$P < 0.01$, ***$P < 0.001$ versus HT29 cells.

LCN2-driven AKT/ERK pathway activation and 5-FU resistance in CRC cells.

LCN2 activates SRC through stabilization of integrin β3

The activity of SRC is positively regulated by autophosphorylation of Tyr416 or negatively regulated by phosphorylation of Tyr527 [30]. LCN2 did not affect SRC phosphorylation on Tyr527 (Fig. 4E), which prompted us to consider that LCN2 might promote SRC autophosphorylation in CRC cells. Integrin β3 can promote SRC Tyr416 phosphorylation by increasing the accumulation of SRC in the cell membrane [31]. Confocal imaging showed that most of the SRC in HT29R cells was distributed in the cell membrane, unlike in HT29 cells (Fig. 5A). Coincidentally, the integrin β3 protein level was increased in HT29R cells (Fig. 5B; Supplementary Fig. S6A). Moreover, knocking down LCN2 expression in HT29R and SW480 cells resulted in a significant reduction in the integrin

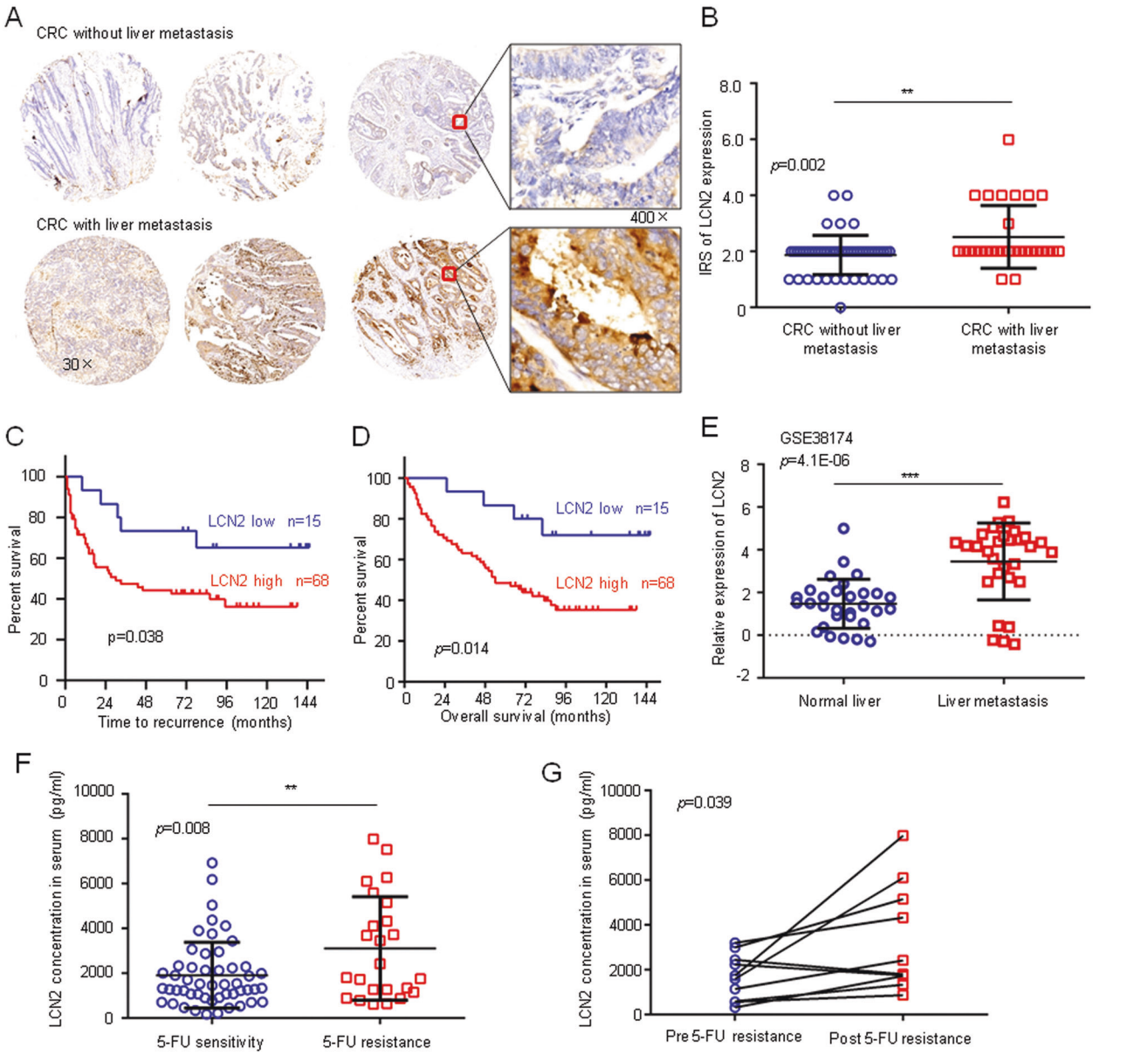

Fig. 2 LCN2 expression is associated with liver metastasis, recurrence, and prognosis in patients with CRC. A The protein expression of LCN2 in CRC patients was determined by IHC. A tissue microarray containing 83 primary human CRC specimens was used to evaluate the LCN2 protein level. Representative images of three specimens from patients with or without liver metastasis are presented (left). The indicated areas were enlarged (right). **B** The IRS for LCN2 in CRC primary tumors from patients with or without liver metastasis were calculated. **C, D** Kaplan–Meier analysis of progression-free survival/overall survival times in 83 CRC patients according to the LCN2 protein IRS. High LCN2 expression was defined as an IRS > 1. **E** LCN2 mRNA levels in CRC with or without liver metastasis from the GSE38174 cohort were calculated. **F** Serum levels of LCN2 in CRC patients with or without recurrence following 5-FU treatment were determined by ELISA. **G** Serum levels of LCN2 in ten CRC patients pre and post recurrence following 5-FU treatment were measured by ELISA. $^{**}P < 0.01$, $^{***}P < 0.001$.

β3 level, while overexpression of LCN2 in RKO cells increased the integrin β3 level (Fig. 5C; Supplementary Fig. S6B). These results suggest that integrin β3 may be involved in LCN2-mediated SRC (Tyr416) phosphorylation. Indeed, knockdown of integrin β3 not only reduced the phosphorylation level of SRC (Tyr416), ERK, and AKT in SW480 cells but also completely blocked the aberrant phosphorylation of SRC (Tyr416), ERK, and AKT in HT29R cells (Fig. 5D; Supplementary Fig. S6C). Moreover, the increased p-SRC (Tyr416) in HT29R cells was distributed mainly at the cell membrane, and this localization was completely abolished by interference with integrin β3 expression (Fig. 5E). These results suggest that LCN2 enhances the distribution of SRC at the cell membrane via integrin β3, resulting in autophosphorylation of SRC on Tyr416. Ectopically expressed LCN2 and endogenous integrin β3 coimmunoprecipitated together in both HT29 and RKO cells (Fig. 5F), and partial colocalization of LCN2 and integrin β3 was observed at the cytomembrane of CRC cells (Fig. 5G). To prove a direct interaction, we performed a pulldown experiment using LCN2 protein and found that purified LCN2 pulled down integrin β3 in cell lysate (Fig. 5H). When tripeptide IDG, a recognition motif of integrin on LCN2, was mutated into IAD, integrin β3 was unable to bind to the LCN2 mutant (ΔLCN2) (Fig. 5I). These results indicate that LCN2 directly binds to the integrin β3 protein as a ligand. The ubiquitination assay showed that the level of ubiquitinated integrin β3 was markedly decreased in HT29R cells compared with HT29 cells (Fig. 5J). In addition,

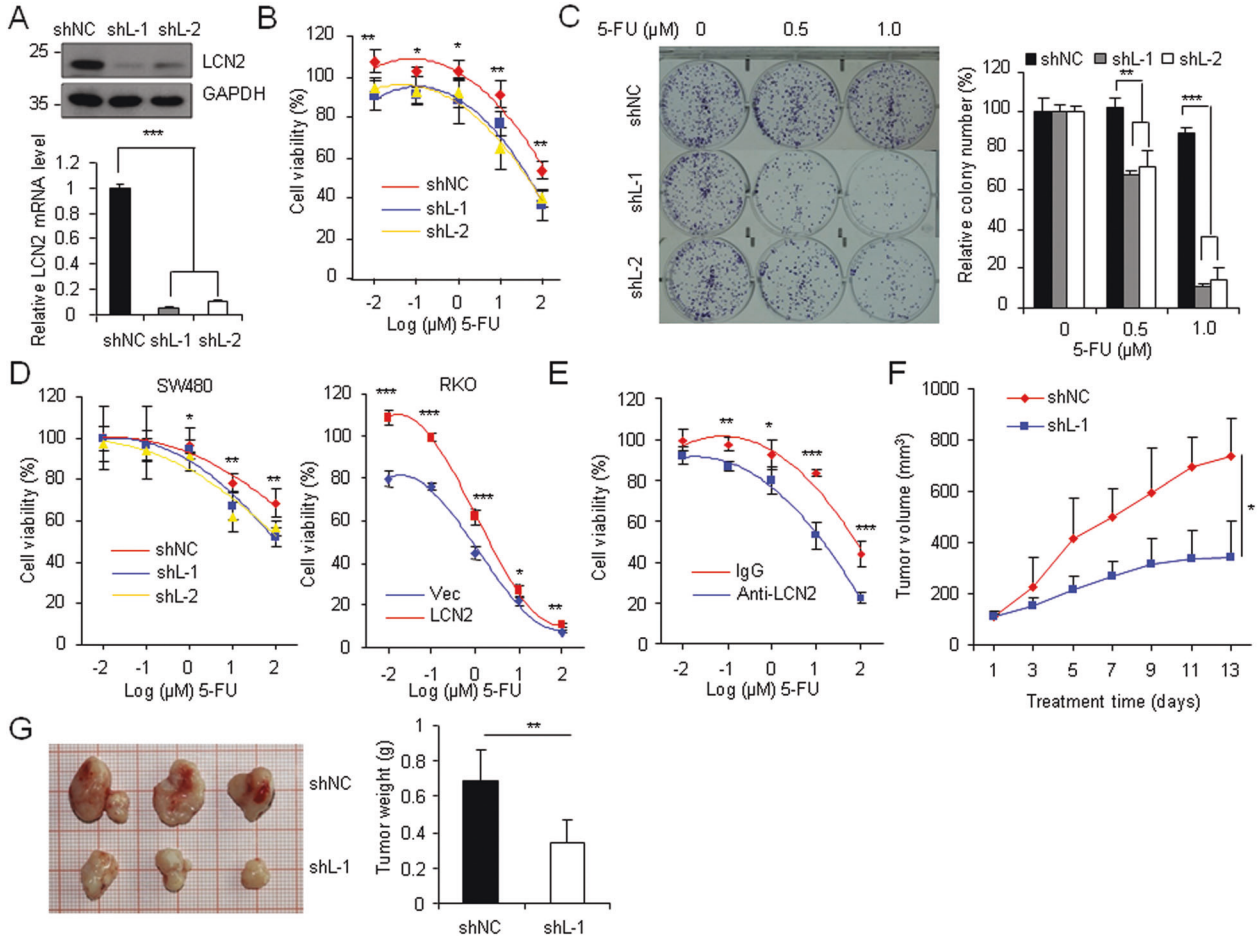

Fig. 3 LCN2 confers 5-FU resistance on CRC cells. A Knockdown of LCN2 in HT29R cells was verified by qRT-PCR and western blot analysis. HT29R cells were infected with shLCN2 (shL-1, shL-2) or nontargeted (shNC) lentivirus for 72 h. **B**, **C** Knockdown of LCN2 resensitized HT29R cells to 5-FU. Lentivirus-infected cells were treated with 5-FU, and cell viability was assessed by MTT and clonogenic assays. **D** Knocking down LCN2 expression in SW480 cells increased 5-FU cytotoxicity (left), while ectopic overexpression of LCN2 in RKO cells reduced 5-FU cytotoxicity (right). Cell viability was assessed by an MTT assay. SW480 cells infected with shLCN2 (shL-1, shL-2) or nontargeted (shNC) lentivirus and RKO cells stably overexpressing LCN2 or empty vector (Vec) were treated with 5-FU (0.01–100 μM) for 72 h. **E** Inhibition of LCN2 by treatment with an anti-LCN2 antibody enhanced the sensitivity of HT29R cells to 5-FU. Cell viability was assessed by an MTT assay. HT29R cells were treated with the indicated concentrations of 5-FU (0.01–100 μM) and/or the anti-LCN2 antibody. **F**, **G** Suppression of LCN2 expression restored the sensitivity of HT29R cells to 5-FU in vivo. HT29R cells stably transfected with shLCN2 (shL-1) or the nontargeted shRNA (shNC) were inoculated subcutaneously into mice, and tumor-bearing mice were intraperitoneally treated with 50 mg/kg doses of 5-FU. Tumor size was measured every other day (**F**). Tumors from euthanized mice were excised, photographed, and weighed. Representative images of the xenograft tumors are shown (**G**). The volumes and weights of xenograft tumors ($n = 3$) were determined and are shown as the mean ± SD values. *$P < 0.05$, **$P < 0.01$, ***$P < 0.001$.

silencing LCN2 in HT29R and SW480 cells obviously promoted the ubiquitination of integrin β3, while overexpression of LCN2 in RKO cells inhibited the ubiquitination of integrin β3 (Fig. 5K, Supplementary Fig. 6D). Taken together, these results indicate that the interaction between LCN2 ligand and integrin β3 prevents the ubiquitination-mediated degradation of integrin β3 and increases the distribution of integrin β3 at the cytomembrane, thus recruiting more SRC to the cytomembrane for autoactivation.

LCN2 expression is elevated through epigenetic changes and LCN2/NF-κB feedback

Epigenetic modifications are a critical cause of therapeutic resistance [32]. Treatment with 5-Aza-dC markedly increased the mRNA expression of LCN2 in both HT29 and RKO cells (Fig. 6A). These data prompted us to consider that the upregulation of LCN2 in HT29R cells might be caused by DNA demethylation after sustained drug exposure. Careful examination of the LCN2 promoter region showed that it contains several CpG sites (Fig. 6B). Moreover, bisulfite sequencing demonstrated that LCN2 promoter CpG sites were hypermethylated in HT29 cells, while most CpG sites were demethylated in HT29R cells (Fig. 6C). These results suggest that promoter DNA demethylation contributes to LCN2 overexpression in HT29R cells. In HT29R cells, NF-κB signaling was activated, and inhibition of LCN2 expression significantly attenuated NF-κB activity in this cell line (Fig. 6D, E). Furthermore, manipulation of LCN2 expression also changed modified NF-κB activity in SW480 and RKO cells (Fig. 6E; Supplementary Fig. S6E). These results suggest that LCN2 is an activator of NF-κB in CRC cells. Intriguingly, we identified an NF-κB-binding site in the promoter of the LCN2 gene and found that the hypermethylated CpG249 site in the NF-κB-binding region was completely demethylated in HT29R cells. Moreover, LCN2 expression was dose-dependently inhibited by treatment with the NF-κB inhibitor (PDTC) (Fig. 6B, C, F). Taken together, these results suggest that a positive feedback loop is formed between LCN2 and NF-κB and that epigenetic induction of LCN2 activates this LCN2/NF-κB feedback loop, which further amplifies the expression of LCN2.

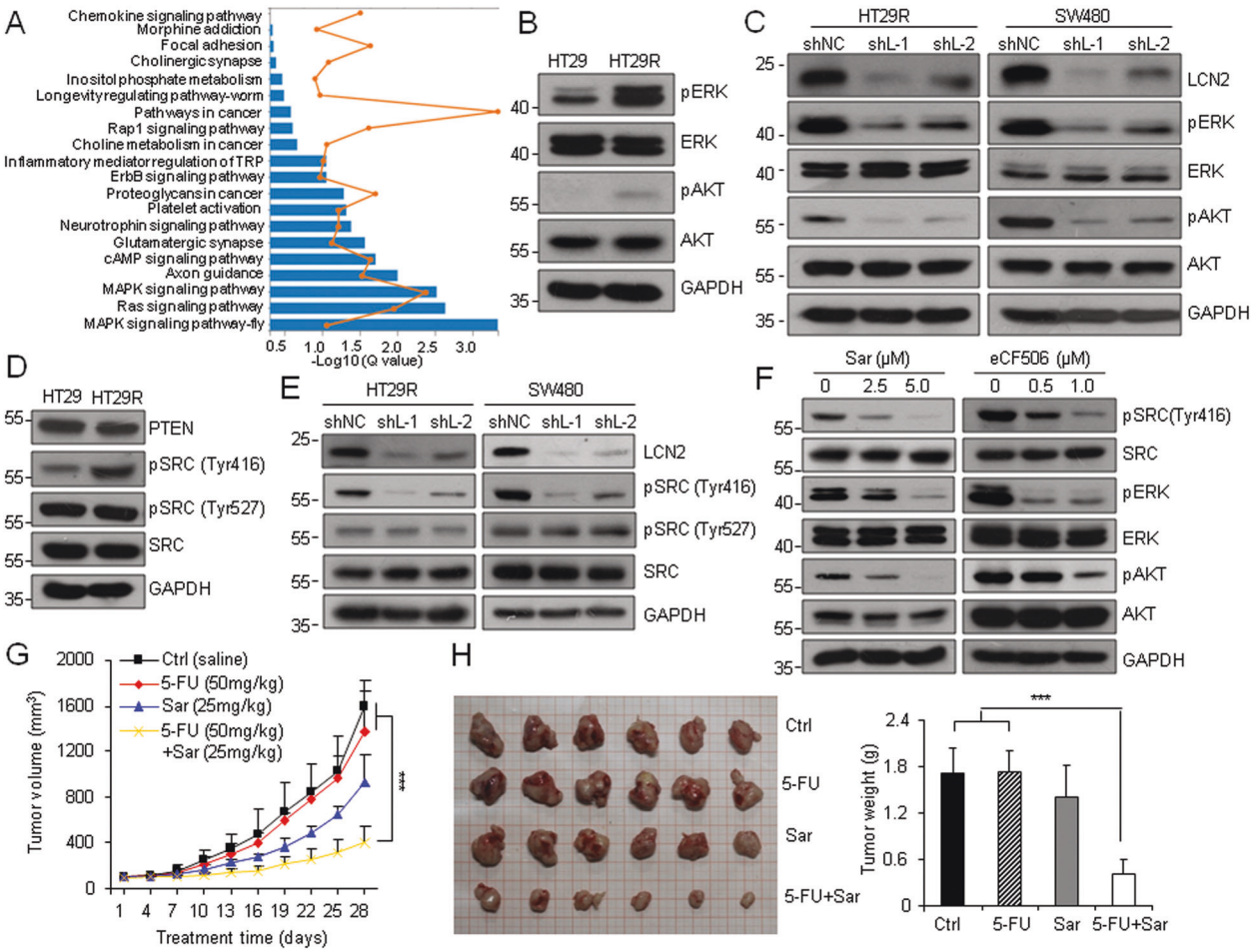

Fig. 4 LCN2 drives 5-FU resistance in CRC cells through SRC-mediated AKT/ERK cascades. A Enrichment analysis results of KEGG pathways changed in HT29R cells. **B** The levels of phosphorylated AKT and ERK in HT29 and HT29R cells were determined by western blot analysis. **C** The effects of LCN2 knockdown on the activation of AKT and ERK were evaluated. HT29R cells and SW480 cells were infected with shLCN2 (shL-1, shL-2) or nontargeted (shNC) lentivirus for 72 h. **D** Phosphorylation of SRC was analyzed by western blot. Phosphorylated SRC at Tyr416, p-SRC Y416; phosphorylated SRC at Tyr527, p-SRC Y527. **E** Knockdown of LCN2 reduced the level of phosphorylated SRC (Tyr416) in HT29R and SW480 cells. **F** The effect of the SRC inhibitor saracatinib (Sar) and eCF506 on the phosphorylation of AKT and ERK in HT29R cells. Cells were treated with DMSO, 2.5 and 5.0 μM Sar or 0.5 and 1.0 μM eCF506 for 48 h. **G**, **H** Combination treatment with 5-FU and Sar synergistically inhibited tumor growth in nude mice. Mice bearing HT29R tumors were treated with control (saline, Ctrl), 5-FU, Sar, or 5-FU plus Sar at the indicated doses. Tumor size was measured every 3 days (**G**). Tumors were excised, photographed, and weighed (**H**). Representative images of xenograft tumors are shown (left). The tumor weights were determined and are shown as the mean ± SD values (right, $n = 6$). ***$P < 0.001$.

DISCUSSION

Resistance to 5-FU is a major cause of therapeutic failure in patients with CRC [33]. The discovery of novel 5-FU resistance drivers and underlying mechanisms would be helpful for the development of therapeutic strategies to overcome 5-FU resistance in CRC patients. In this study, we found that LCN2 was markedly upregulated in CRC cells with acquired 5-FU resistance and was associated with metastasis, recurrence, and survival in CRC patients. Our data demonstrated that LCN2 greatly decreased the cytotoxic effect of 5-FU and functioned as a driver of 5-FU resistance in CRC. Mechanistically, the physical interaction between LCN2 and integrin β3 increased the stability of integrin β3, resulting in enhanced SRC recruitment to the cytomembrane for autophosphorylation. In turn, activation of SRC led to increased phosphorylation of AKT/ERK, thus activating the AKT/ERK-mediated antiapoptotic program. In addition, we found that LCN2 promoter demethylation increased LCN2 expression in CRC cells with acquired 5-FU resistance. LCN2 is an activator of NF-κB, and inhibition of NF-κB reduced LCN2 expression. Based on our results, we propose a novel LCN2-driven 5-FU resistance mechanism (Fig. 7). In brief, in CRC cells subjected to sustained treatment with 5-FU, the increase in LCN2 expression caused by epigenetic changes activates the LCN2/NF-κB feedback loop, thus further promoting the expression of LCN2, which activates SRC/AKT/ERK cascades by interacting with integrin β3, leading to the development of acquired 5-FU resistance.

In this study, we identified LCN2 as a new driver of acquired 5-FU resistance in CRC. Previous studies have shown that LCN2 can affect sensitivity to certain anticancer drugs, such as vincristine and TRAIL, but the mechanisms involved are poorly understood [26, 28]. Moreover, the consequence of high LCN2 expression on 5-FU resistance in CRC has not been previously reported. Here, we found that the expression of LCN2 was significantly upregulated in 5-FU-resistant cells and in metastatic lesions of CRC patients. CRC liver metastasis often implies the development of chemoresistance, and 50% of patients with metastatic CRC exhibit resistance to 5-FU-based chemotherapy [34]. Our data demonstrated that overexpression of LCN2 induced 5-FU resistance by activating SRC via Tyr416 phosphorylation. We further revealed that hyperactivation of SRC enhanced the antiapoptotic ability of CRC cells by activating downstream AKT/ERK cascades, thus providing an alternate survival pathway. The

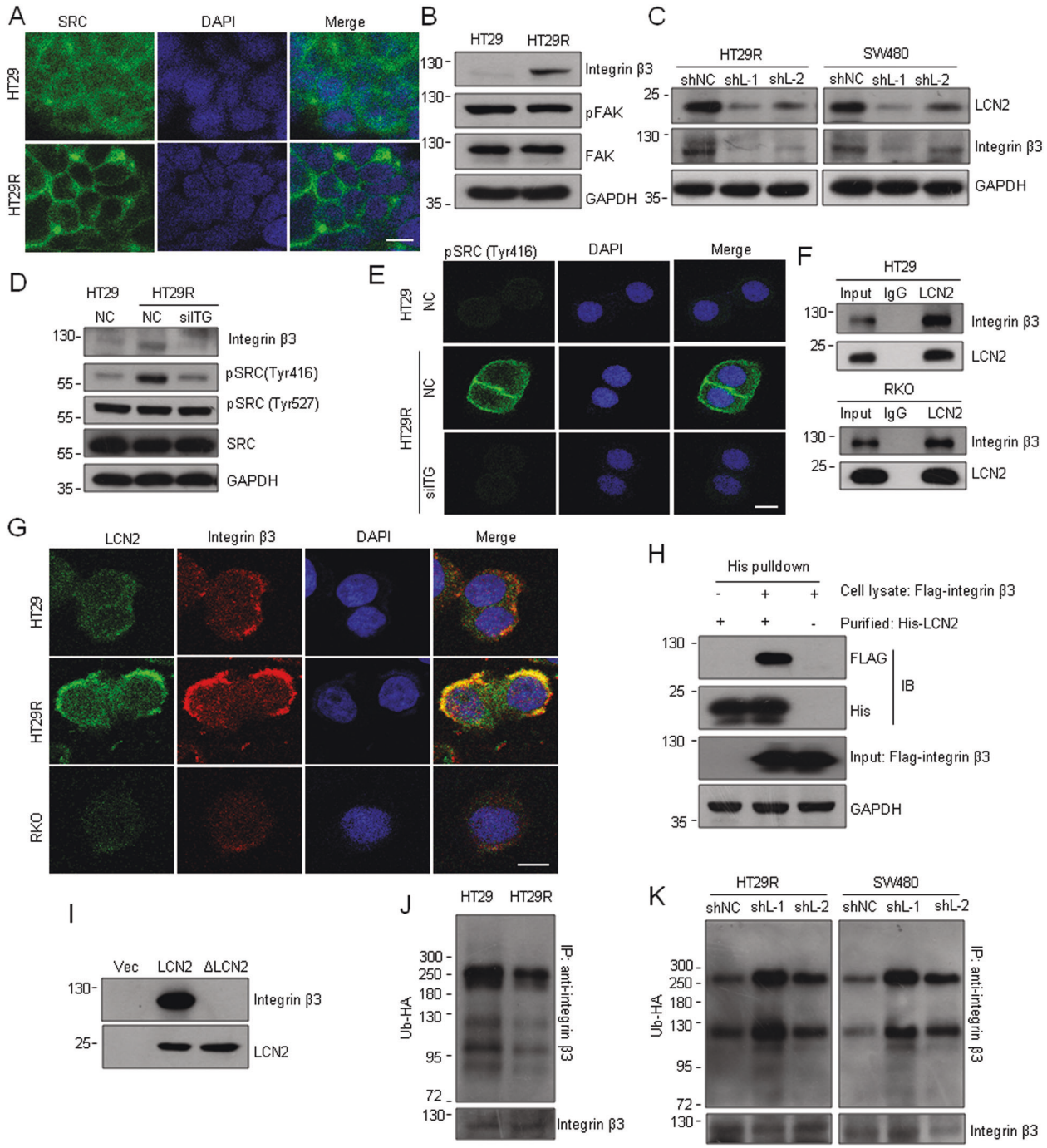

Fig. 5 The LCN2-integrin β3 interaction recruits SRC to the cytomembrane for phosphorylation. A The distribution of SRC in HT29 and HT29R cells was evaluated by immunofluorescence staining and confocal microscopy imaging. Scale bar, 10 μm. **B** Integrin β3 expression was elevated in HT29R cells. Western blot analysis of integrin β3 and FAK levels in HT29 and HT29R cells. **C** Knockdown of LCN2 suppressed integrin β3 expression. HT29R cells and SW480 cells were infected with shLCN2 (shL-1, shL-2) or nontargeted (shNC) lentivirus for 72 h. **D** Knockdown of integrin β3 abolished the hyperactivation of SRC (Y416) in HT29R cells. Cells were transfected with a nontargeted control siRNA (NC) or a siRNA against integrin β3 (siITG). **E** Phosphorylated SRC (Y416) was detected by immunofluorescence staining and confocal microscopy imaging. Scale bar, 10 μm. Cells were transfected with a nontargeted control siRNA (NC) or a siRNA against integrin β3 (siITG). Scale bar, 10 μm. **F** Co-immunoprecipitation was performed to analyze the physical interaction between LCN2 and integrin β3. **G** The colocalization of LCN2 and integrin β3 at the cytomembrane in HT29, HT29R, and RKO cells was imaged by confocal microscopy. Scale bar, 10 μm. **H** Pulldown assay was performed to analyze the direct interaction between LCN2 and integrin β3. Purified His-tagged LCN2 protein was used to pulldown Flag-tagged integrin β3 from cell lysate of HEK293T cells. **I** Co-immunoprecipitation was performed to analyze the interaction between integrin β3 and LCN2 or IDG motif mutated LCN2 (ΔLCN2). **J** Ubiquitination assay of integrin β3 in HT29 and HT29R cells. **K** Effects of LCN2 knockdown on the ubiquitination of integrin β3. HT29R and SW480 cells were infected with shLCN2 (shL-1, shL-2) or nontargeted (shNC) lentivirus for 72 h.

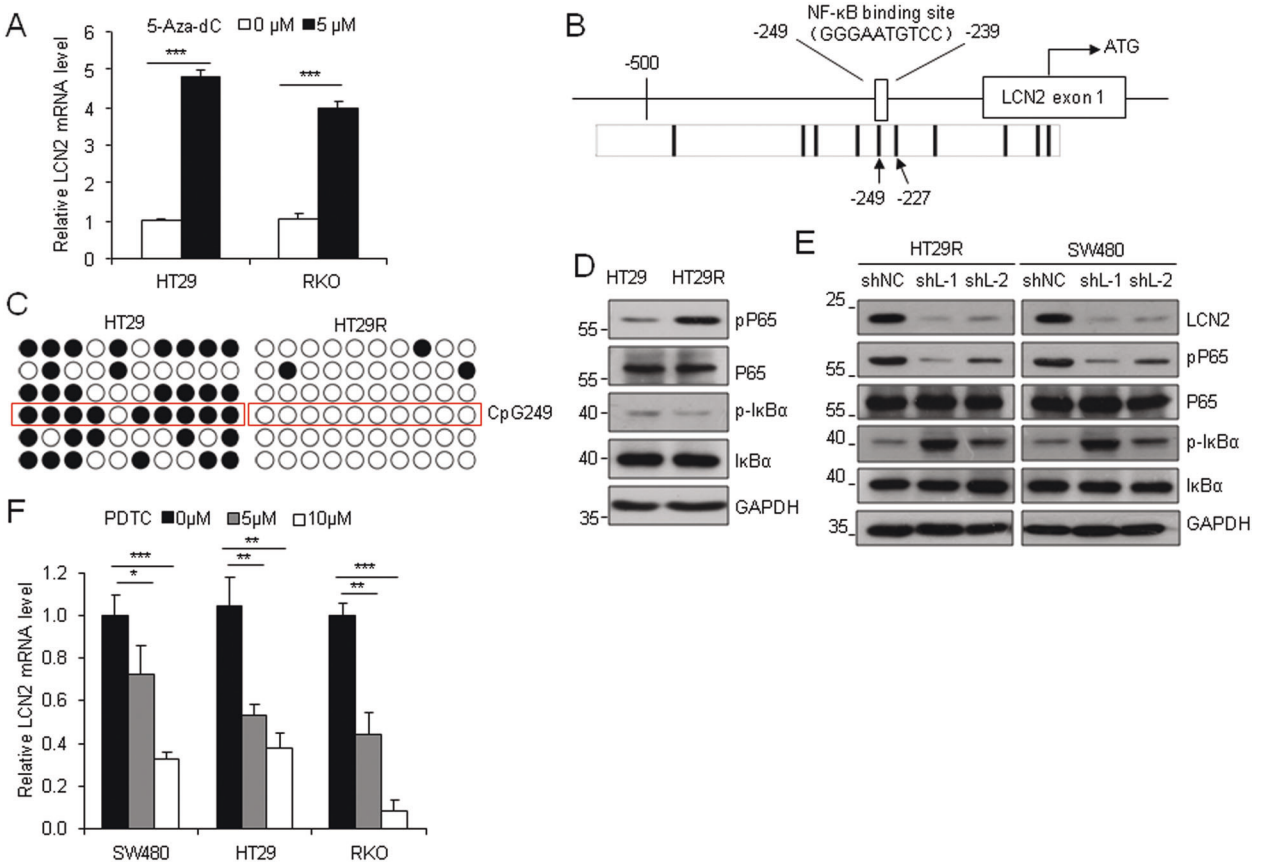

Fig. 6 LCN2 expression is elevated through promoter CpG demethylation and LCN2/NF-κB feedback. A HT29 and RKO cells were treated with 5 μM 5-aza-2′-deoxycytidine (5-Aza-dC) for 3 days, and the LCN2 mRNA level was determined using qRT-PCR. The data are shown as the mean ± SD values. **B** Schematic representation of the CpG sites and NF-κB-binding site in the LCN2 promoter region. **C** Bisulfite sequencing of the LCN2 promoter in HT29 and HT29R cells. The open and filled circles represent unmethylated and methylated CpG sites, respectively. Each line represents a single clone. **D** NF-κB activity was assessed in HT29 and HT29R cells by western blot analysis. **E** Knockdown of LCN2 attenuated the activity of NF-κB in CRC cells. HT29R cells and SW480 cells were infected with shLCN2 (shL-1, shL-2) or nontargeted (shNC) lentivirus for 72 h. **F** Inhibition of NF-κB reduced the expression of LCN2 in CRC cells. Cells were treated with the indicated concentration of PDTC for 72 h, and LCN2 mRNA levels were determined by qRT-PCR. In **A**, **F**, the error bars indicate the SD of three independent experiments. $^{*}P < 0.05$, $^{**}P < 0.01$, $^{***}P < 0.001$ versus control.

proto-oncogene SRC is a non-receptor tyrosine kinase that plays a key role in the regulation of essential cellular processes such as morphological processes, differentiation, proliferation, and survival [35]. SRC facilitates the activation of signal transduction pathways (PI3K/AKT, MAPK, and β-catenin/E-cadherin complex signaling) and transcription factors (STAT3 and STAT5b) [36]. SRC is overexpressed in ~70% of human colon cancers, and high expression and activity of SRC correlates with aggressive clinical features such as cancer cell proliferation, invasion, and metastasis [37, 38]. SRC activation has also been reported to be associated with drug resistance in CRC [37]. Dasatinib, a Src inhibitor, sensitizes liver metastatic colorectal carcinoma to oxaliplatin in tumors with high levels of phospho-Src [39]; dasatinib also sensitizes KRAS mutant colorectal tumors to cetuximab [40]. In our study, we showed that the combination of another SRC inhibitor, saracatinib, with 5-FU reversed the 5-FU resistance of CRC cells both in vitro and in vivo. Furthermore, we found that treatment with an anti-LCN2 antibody partially restored the sensitivity of 5-FU-resistant cancer cells to 5-FU. These results suggest that directly targeting LCN2 or indirectly targeting downstream SRC activity is a strategy for overcoming LCN2-mediated 5-FU resistance.

SRC activation is tightly regulated by phosphorylation/dephosphorylation processes. Phosphorylation of the Tyr527 residue keeps SRC in an inactive configuration, and dephosphorylation of the Tyr527 residue results in its activation by autophosphorylation of Tyr416 [41]. Inactive SRC translocates to the cytomembrane, which triggers autophosphorylation at Tyr416 [42]. In this study, we found that LCN2 did not affect the dephosphorylation of SRC Tyr527, but induced autophosphorylation of SRC with integrin-mediated membrane translocation. Integrin is the upstream mediator of SRC and can bind and recruit SRC to the cytomembrane, leading to SRC autophosphorylation on Tyr416. Integrin-mediated SRC priming and activation are associated with tumor proliferation, migration, and chemoresistance [43, 44]. Our data indicate that in CRC cells with acquired 5-FU resistance, LCN2 increased not only the total amount of integrin β3 but also its accumulation at the cytomembrane. Furthermore, our data showed that there has direct physical interaction between LCN2 and integrin β3, while disruption of LCN2 promotes the ubiquitination-mediated degradation of integrin β3. These results suggest that LCN2 can act as a ligand of integrin β3, and the binding of LCN2 to integrin β3 enhances the stability of integrin β3. In summary, our study reveals a novel mechanism of LCN2-mediated SRC activation: the LCN2-integrin β3 interaction enhances the amount and cytomembrane distribution of integrin β3, thereby enhancing the recruitment of SRC to the inner surface of the cell membrane for autoactivation.

LCN2 has been utilized as a blood biomarker in patients with renal injury, inflammatory conditions, and metabolic diseases

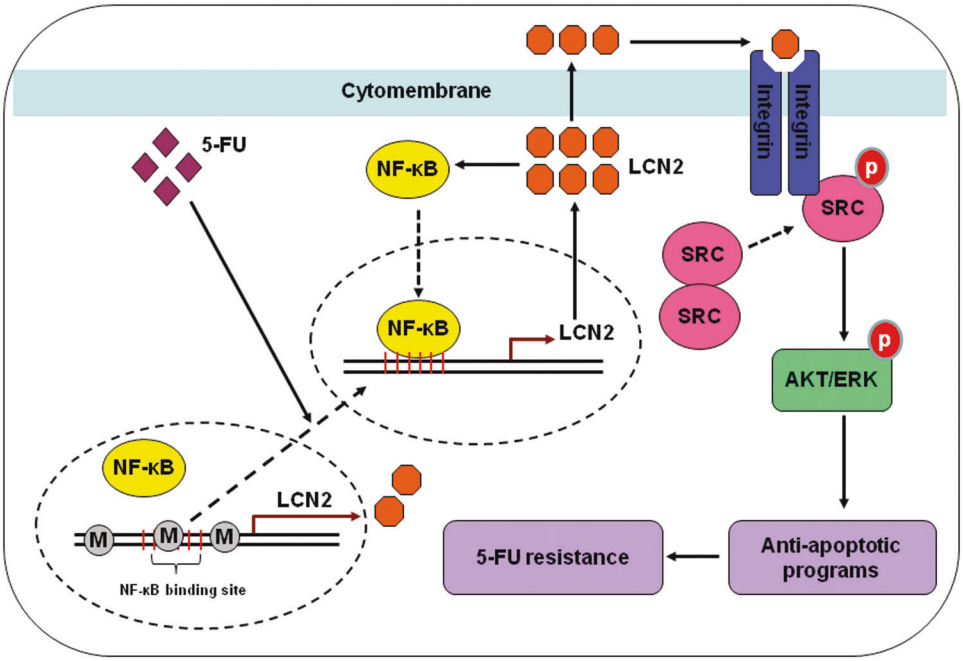

Fig. 7 Proposed molecular mechanism. A model depicting the mechanism by which LCN2 induces acquired 5-FU resistance in CRC.

[14, 20]. We found that LCN2 was upregulated in 5-FU-resistant CRC cells and associated with metastasis and recurrence in CRC patients. Our study suggests that serum LCN2 can be used as a biomarker for acquired 5-FU resistance that is suitable for clinical testing. In the present study, we found that aberrant overexpression of LCN2 results from CpG demethylation of its promoter. Epigenetic modifications, such as DNA hypermethylation or hypomethylation in gene promoters, are commonly involved in drug resistance acquisition [45]. The LCN2 promoter region contains multiple CpG sites, and a demethylated status of the LCN2 promoter has been reported to be associated with an aggressive tumor phenotype in breast cancer [46]. Here, we demonstrated by BSP that most CpG sites in the LCN2 promoter were demethylated under conditions of sustained 5-FU treatment. Our results suggest that epigenetic changes are a primary cause of LCN2 overexpression. Intriguingly, we found that the most thoroughly demethylated CpG249 site is located in a NF-κB-binding element. In the human juvenile costal chondrocyte cell line, binding of NF-κB with this response element induced the expression of LCN2 [47]. Consistent with that report, we demonstrated that inhibition of NF-κB markedly reduced LCN2 expression in CRC cells. More importantly, we found that LCN2 in turn enhanced NF-κB activity in CRC cells. In oral squamous cell carcinoma, the study has shown that LCN2 can promote the activation of NF-κB by binding to ribosomal protein S3 (RPS3) and enhanced the interaction between RPS3 and p65 [29]. These results strongly suggest that a positive feedback loop is formed between LCN2 and NF-κB in CRC cells. Combined with our results, we can speculate that epigenetic induction of LCN2 after sustained 5-FU exposure likely reaches the level needed to activate the LCN2/NF-κB positive feedback loop, and demethylation of the CpG249 site further amplifies this response. Activation of the LCN2/NF-κB positive feedback loop commits cells to a self-sustaining mode, and constitutively stimulates the expression of LCN2, resulting in hyperactivation of SRC and its downstream AKT/ERK cascades. Activation of these cascades in turn confers a survival advantage on CRC cells and eventually triggers 5-FU resistance.

In summary, we identified LCN2 as a novel driver gene that contributes to acquired 5-FU resistance in CRC. LCN2 is upregulated in 5-FU-resistant CRC cells due to promoter demethylation and is associated with the survival of CRC patients. LCN2 attenuates the cytotoxicity of 5-FU by activating the SRC-mediated antiapoptotic program. Mechanistically, the physical interaction between LCN2 and integrin β3 enhances the stability of integrin β3 and increases its distribution at the cytomembrane, thus enhancing the recruitment of SRC to the cytomembrane for autophosphorylation. Activation of SRC leads to increased phosphorylation of AKT/ERK, thus initiating the associated cellular antiapoptotic program. Moreover, LCN2 and NF-κB form a positive feedback loop. Targeting LCN2 or the LCN2-mediated SRC pathway compromises the growth of CRC cells with LCN2-induced 5-FU resistance cells. Our findings reveal a novel mechanism of acquired resistance to 5-FU therapy and suggest that LCN2 can be used as a biomarker and/or therapeutic target for advanced CRC.

MATERIALS AND METHODS

Cell lines and cell culture

The CRC cell lines HT29, RKO, and SW480 were purchased from American Type Culture Collection. The cell lines were authenticated using short tandem repeat DNA profiling recently, and no mycoplasma contamination was detected. HT29 and SW480 cells were cultured in McCoy's 5A medium (Gibco) supplemented with 10% fetal bovine serum at 37 °C in 5% CO_2. RKO cells were cultured in DMEM (Gibco) supplemented with 10% fetal bovine serum, 1% nonessential amino acids, and 1% sodium pyruvate at 37 °C in 5% CO_2. To establish HT29 cells with acquired 5-FU resistance, cells were continuously exposed to increasing concentrations of 5-FU (0.01–2 μg/ml) for at least 8 months.

Reagents and antibodies

Antibodies against phosphorylated (p)-SRC (Tyr416) (#6943), p-SRC (Tyr527) (#2105), SRC (#2109), p-ERK (Thr202/Tyr204) (#9101), ERK (#9102), p-AKT (Ser473) (#9271), AKT (#4691), p-p70 S6 Kinase (Thr421/Ser424) (#9204), p70 S6 Kinase (#2708), p-MEK1/2 (ser217/221) (#86128), MEK1/2 (#8727), DYKDDDDK Flag-Tag (#8146), His-Tag (#12698), p-SAPK/JNK (Thr183/Tyr185) (#9255), SAPK/JNK (#9252), p-P38 (Thr180/Tyr182) (#9211), P38 (#8690), p-IκBα (Ser32) (#2859), IκBα (#4812), p-NF-κB pP65 (Ser536) (#3033), NF-κB P65 (#8242), and GAPDH (#2118) were purchased from Cell Signaling Technology. Antibodies against integrin β3 and p-SRC (Tyr416) (sc-81521) were purchased from Santa Cruz Biotechnology. The

antibody against LCN2 (ab206085) was purchased from Abcam. The short hairpin RNAs (shRNAs) and small interfering RNAs (siRNAs) were purchased from GenePharma (Shanghai, China). The target sequences of the shRNAs against LCN2 and the oligo sequences of the siRNAs against integrin β3 are listed in Supplementary Table S1. Saracatinib (Sar, AZD0530) (a SRC inhibitor), U0126 (an ERK inhibitor), LY294002 (an AKT inhibitor), 5-FU, 3-(4,5-dimethylthiazol-2-yl)−2,5-diphenyltetrazolium bromide (MTT), pyrrolidine dithiocarbamate (PDTC) and 5-aza-2′-deoxycytidine (5-Aza-dC) were purchased from Sigma-Aldrich (USA). eCF506 (a SRC inhibitor), Trametinib (GSK1120212) (an ERK inhibitor), and Pictilisib (GDC0941) (an AKT inhibitor) were purchased from Selleck (USA). Recombinant Human Lipocalin-2/His-tagged Protein (#1757-LC) was purchased from R&D Systems (USA).

Plasmid and transfection

The full-length human LCN2 cDNA was amplified from HEK293 cells using a One-Step RT-PCR System Kit (Invitrogen), subcloned into pcDNA3.1 vector (Invitrogen), and verified by DNA sequencing. Mutagenesis of LCN2 (ΔLCN2) cDNA to change motif ^{176}IDG^{178} into IAD was obtained by direct PCR amplification from LCN2 cDNA. Flag-tagged integrin β3 expression plasmid was purchased from Miaoling Biotech. (China). Transfections were performed using Lipofectamine 2000 reagent (Invitrogen) according to the manufacturer's instructions. To obtain stable transfectants, transfected cells were cultured in a medium containing G418, and resistant clones were confirmed by western blot analysis.

RNA sequencing

Total RNA was isolated from HT29 and HT29R cell lines using TRIZOL reagent (Invitrogen). RNAs were reverse transcribed to cDNA. cDNAs were amplified and fragmented. The final products were sequenced using the Illumina HiSeq 4000 or X Ten platform (BGI-Shenzhen, China). The RNA-seq (RNA-sequencing) data are available under NCBI Bioproject PRJNA706856. The sequencing data were filtered with SOAPnuke (https://github.com/BGI-flexlab/SOAPnuke). The clean reads were mapped to the reference genome using HISAT2 (http://www.ccb.jhu.edu/software/hisat/index.shtml). Bowtie2 (http://bowtiebio.sourceforge.net/%20Bowtie2%20/index.shtml) was used to align the clean reads to the reference coding gene set. RSEM (https://github.com/deweylab/RSEM) was then used to calculate gene expression levels. The pheatmap package (https://cran.r-project.org/web/packages/pheatmap/index.html) was used to generate a heatmap based on the gene expression levels in the two compared cell lines. DESeq2 (http://www.bioconductor.org/packages/release/bioc/html/DESeq2.htm) was used to perform differential expression analysis. Phyper (https://en.wikipedia.org/wiki/Hypergeometric_distribution) was used to perform KEGG enrichment analysis of annotated differentially expressed genes based on the results of a hypergeometric test.

MTT and clonogenic assays

Cell viability was analyzed by an MTT assay as described previously [48]. For the clonogenic assay, 1×10^3 cells were seeded in six-well plates in triplicate and incubated overnight. After treatment with the indicated concentrations of drugs for 48 h, cells were cultured in drug-free medium for 12–14 days. At the end of the experiment, colonies were stained with 0.5% crystal violet, and colonies with ≥50 cells were counted.

Xenograft assay

All animals were used in accordance with the guidelines of the Institutional Animal Care and Use Committee of Wenzhou Medical University (WYDW2019-0842). Six-week-old male athymic nude (nu/nu) mice were purchased from Vital River Experimental Animal Center (Beijing, China) and maintained under pathogen-free conditions. To verify the function of LCN2 in the growth of 5-FU-resistant CRC, mice were randomly divided into two groups. HT29R cells (2×10^6) stably infected with the indicated shLCN2 or shNC lentivirus (GeneChem Co. Shanghai, China) were suspended in 100 µl of PBS and subcutaneously injected into the dorsal flanks of mice. When the mean tumor volume reached 100 mm^3, the mice were intraperitoneally injected with 50 mg/kg 5-FU every 2 days for 2 weeks. To evaluate the therapeutic effect of saracatinib treatment in 5-FU-resistant CRC, HT29R cells (2×10^6 cells/100 µl) were inoculated into the right dorsal flanks of mice by subcutaneous injection. When the tumor volume reached approximately 100 mm^3, tumor-bearing mice were randomly divided into four groups ($n = 6$) and treated with (1) saline (the control group), (2) 5-FU (50 mg/kg intraperitoneally every 2 days for 2 weeks) alone, (3) saracatinib (25 mg/kg orally every three days for a total of 4 weeks), or (4) the combination of 5-FU and saracatinib. Tumors were measured every 2 or 3 days, and the tumor volume was calculated with the following formula: length (mm) × width^2 (mm^2) × 0.5326. At the end of the experiments, mice were euthanized, and tumors were harvested, weighted, and extracted for preparation of protein lysates.

Western blot analysis

Protein levels were determined by western blot analysis as described previously [48]. Proteins were separated using sodium dodecyl sulfate-polyacrylamide gel electrophoresis (SDS-PAGE) and transferred to polyvinylidene difluoride membranes (Bio-Rad). After blocking in 5% milk in TBST (containing 0.1% Tween 20), membranes were incubated first with primary antibodies (1:500–1,000) and then with horseradish peroxidase (HRP)-conjugated secondary antibodies. Protein bands were visualized with an Immun-Star HRP Chemiluminescence Kit (Bio-Rad).

Apoptosis analysis

The apoptosis assay was performed via flow cytometry as described previously [49]. An Annexin V-FITC/Propidium Iodide Apoptosis Detection Kit (BD Biosciences, USA) was used in accordance with the manufacturer's instructions. After treatment with 5-FU, CRC cells were harvested, washed twice with cold PBS, and resuspended in 1× binding buffer. Next, cells were incubated with 5 µl of Annexin V-FITC and 5 µl of propidium iodide for 15 min at room temperature in the dark. The relative percentages of apoptotic cells were analyzed with a NOVE flow cytometer (BD Biosciences). All experiments were performed in triplicate.

Quantitative real-time PCR (qRT-PCR)

qRT-PCR was performed as described previously [48]. Total RNA was isolated from CRC cell lines and tumor samples using TRIZOL reagent (Invitrogen). A total of 2 µg of total RNA was reverse transcribed to cDNA with M-MLV reverse transcriptase (Invitrogen), and each cDNA sample was analyzed in triplicate in an Applied Biosystems 7500 quantitative real-time PCR system (Applied Biosystems, USA) with SYBR Green (Tiangen, China) according to the manufacturer's protocol. An endogenous housekeeping gene (GAPDH) was used as the internal control. The thermal cycling conditions were as follows: 95 °C for 2 min, followed by 40 cycles at 95 °C for 15 s, 60 °C for 30 s and 68 °C for 30 s. The primer sequences are listed in Supplementary Table S2. Relative quantification of mRNA levels was performed using the comparative threshold cycle (C_t) method. When necessary, we converted the $\Delta\Delta C_t$ values to expression fold change values using the formula $2^{-\Delta\Delta Ct}$.

Co-immunoprecipitation (Co-IP)

Immunoprecipitation was performed as described previously [50]. Cells were washed with ice-cold PBS and lysed in immunoprecipitation assay buffer (50 mM Tris/HCl (pH 7.5), 150 mM NaCl, 1% Triton X-100, 1 mM EDTA, and 10% glycerol) supplemented with Protease/Phosphatase Inhibitor Cocktail (Cell Signaling Technology). Lysates were incubated on ice for 20 min and centrifuged at 12,000 rpm for 20 min at 4 °C. Cell lysates were incubated first with the corresponding primary antibody overnight at 4 °C and then with Protein G-Sepharose (GE Healthcare) for 3 h at 4 °C. The beads were washed four times with immunoprecipitation assay buffer, suspended in Laemmli buffer, and boiled for 5 min. Samples were analyzed by western blotting with the indicated antibodies.

Immunofluorescence

Immunofluorescence analysis was performed as described previously [48]. In brief, cells were seeded on coverslips for 48 h. After gentle washes with PBS, cells were fixed with 4% formaldehyde and permeabilized with 0.5% Triton X-100 in PBS. Cells were subsequently blocked with 2% bovine serum albumin in PBS-0.1% Triton X-100 prior to incubation with anti-LCN2 (diluted 1:100), anti-integrin β3 (diluted 1:100), anti-SRC (diluted 1:400), and anti-p-SRC (Tyr416) (diluted 1:400) antibodies at 4°C overnight. After three washes with PBS-0.1% Triton X-100, samples were incubated with Alexa Fluor 488 or 594-conjugated secondary antibodies (diluted 1:500). Coverslips were mounted on glass slides with 4′,6-diamidino-2-phenylindole for nuclear staining, and cell images were acquired with a confocal microscope via Nikon NIS-Elements software.

Ubiquitination assay

The ubiquitination assay was performed as described previously [50]. Cells were transfected with the HA-Ubquitin plasmid. Twenty-four hours after

transfection, cells were treated with the proteasome inhibitor MG132 (25 mM) for 4 h and were then lysed in ubiquitination assay buffer (50 mM Tris/HCl (pH 7.4), 150 mM NaCl, 1 mM EDTA and 1% NP40) containing Protease/Phosphatase Inhibitor Cocktail (Cell Signaling Technology). Cell lysates were clarified and incubated with an anti-integrin β3 antibody overnight at 4 °C. Immunocomplexes were incubated with Protein G-Sepharose (GE Healthcare) for another 3 h at 4 °C, washed four times with wash buffer (50 mM Tris/HCl (pH 7.4), 150 mM NaCl, 1 mM EDTA, and 0.1% NP40), and boiled for 5 min in Laemmli buffer before separation by SDS-PAGE. Western blotting was performed with an anti-HA tag antibody to detect ubiquitinated integrin β3.

Bisulfite sequencing PCR (BSP)

BSP was performed as described previously [48]. Genomic DNA was isolated with a Cell/Tissue DNA Extraction Kit (BioTeke, China), and bisulfite modification of genomic DNA was performed using an EZ DNA Methylation-Gold Kit (Zymo Research Corporation). The primers used for BSP were designed with MethPrimer 2.0 (www.urogene.org/methprimer2/). The sequences of the primers used for BSP are listed in Supplementary Table S2. CpG sites and the BSP products were analyzed with the QUMA program (http://quma.cdb.riken.jp/).

Immunohistochemistry (IHC)

CRC tissue samples with appropriate Institutional Review Board approval and patient-informed consent were obtained from Shanghai GenePharma Co.,Ltd. All patients have received 5-FU based regimen as adjuvant therapy. IHC was performed as described previously [49]. Immunohistochemical staining of tissue microarrays was performed with an antibody against LCN2. After immunohistochemical staining, the tissue microarray chips were digitally scanned, and the levels of LCN2 were scored semiquantitatively based on the staining intensity and distribution to determine the immunoreactive score (IRS). In brief, the final IRS was determined by multiplying the intensity score by the positivity score of the stained cells. The intensity score was assigned as follows: 0 = negative staining, 1 = weak staining, 2 = moderate staining, and 3 = strong staining. The positivity score was defined as follows: 0 = 0%, 1 = 0–25%, 2 = 25–50%, 3 = 50–75%, and 4 = 75–100%.

Pulldown assay

His-tagged LCN2 (R&D Systems#1757-LC) and cell lysate from HEK293T cells overexpressing Flag-tagged Integrin β3 were used to perform His-pulldown experiments, according to the instructions of the Pierce Cobalt kit (PullDown PolyHis Protein: Protein Interaction Kit cat. #21277 from Thermo Fisher). The interacting proteins were analyzed by western blotting. The primary antibodies used were anti-His (CST#12698), anti-FLAG (CST#8146).

ELISA

CRC patient blood samples with appropriate institutional review board approval and patient-informed consent were obtained from the First Affiliated Hospital of Wenzhou Medical University. Serum samples were collected from CRC patients treated with 5-FU and stored at −80 °C. The recurrence/metastasis of tumors was defined as locoregional recurrence, distant metastasis, or both. LCN2 level in serum was measured using the ELISA Kit purchased from BaiAoLaiBo (China).

Statistical analysis

All experiments were repeated at least three times with independent cultures. Statistical analysis was carried out using Student's *t*-test or the Kaplan-Meier method with SPSS 24. A *P* value of less than 0.05 was considered statistically significant. Significance levels are labeled in the figures as follows: $*P < 0.05$; $**P < 0.01$; and $***P < 0.001$.

REFERENCES

1. Bray F, Ferlay J, Soerjomataram I, Siegel RL, Torre LA, Jemal A. Global cancer statistics 2018: GLOBOCAN estimates of incidence and mortality worldwide for 36 cancers in 185 countries. CA Cancer J Clin. 2018;68:394–424.
2. Chen L, She X, Wang T, He L, Shigdar S, Duan W, et al. Overcoming acquired drug resistance in colorectal cancer cells by targeted delivery of 5-FU with EGF grafted hollow mesoporous silica nanoparticles. Nanoscale. 2015;7:14080–92.
3. Longley DB, Harkin DP, Johnston PG. 5-fluorouracil: mechanisms of action and clinical strategies. Nat Rev Cancer. 2003;3:330–8.
4. Blondy S, David V, Verdier M, Mathonnet M, Perraud A, Christou N. 5-Fluorouracil resistance mechanisms in colorectal cancer: from classical pathways to promising processes. Cancer Sci. 2020;111:3142–54.
5. Wang TL, Diaz LA Jr, Romans K, Bardelli A, Saha S, Galizia G, et al. Digital karyotyping identifies thymidylate synthase amplification as a mechanism of resistance to 5-fluorouracil in metastatic colorectal cancer patients. Proc Natl Acad Sci USA 2004;101:3089–94.
6. Salonga D, Danenberg KD, Johnson M, Metzger R, Groshen S, Tsao-Wei DD, et al. Colorectal tumors responding to 5-fluorouracil have low gene expression levels of dihydropyrimidine dehydrogenase, thymidylate synthase, and thymidine phosphorylase. Clin Cancer Res. 2000;6:1322–7.
7. Wang H, Li JM, Wei W, Yang R, Chen D, Ma XD, et al. Regulation of ATP-binding cassette subfamily B member 1 by Snail contributes to chemoresistance in colorectal cancer. Cancer Sci. 2020;111:84–97.
8. Wilson BJ, Schatton T, Zhan Q, Gasser M, Ma J, Saab KR, et al. ABCB5 identifies a therapy-refractory tumor cell population in colorectal cancer patients. Cancer Res. 2011;71:5307–16.
9. Violette S, Poulain L, Dussaulx E, Pepin D, Faussat AM, Chambaz J, et al. Resistance of colon cancer cells to long-term 5-fluorouracil exposure is correlated to the relative level of Bcl-2 and Bcl-X(L) in addition to Bax and p53 status. Int J Cancer. 2002;98:498–504.
10. Tominaga T, Iwahashi M, Takifuji K, Hotta T, Yokoyama S, Matsuda K, et al. Combination of p53 codon 72 polymorphism and inactive p53 mutation predicts chemosensitivity to 5-fluorouracil in colorectal cancer. Int J Cancer. 2010;126:1691–701.
11. Pothuraju R, Rachagani S, Krishn SR, Chaudhary S, Nimmakayala RK, Siddiqui JA, et al. Molecular implications of MUC5AC-CD44 axis in colorectal cancer progression and chemoresistance. Mol Cancer. 2020;19:37–01156.
12. de la Cruz-Morcillo MA, Valero ML, Callejas-Valera JL, Arias-GonzÃ¡lez L, Melgar-Rojas P, GalÃ¡n-Moya EM, et al. P38MAPK is a major determinant of the balance between apoptosis and autophagy triggered by 5-fluorouracil: implication in resistance. Oncogene. 2012;31:1073–85.
13. Zou ZW, Chen HJ, Yu JL, Huang ZH, Fang S, Lin XH. Gap junction composed of connexin43 modulates 5 fluorouracil, oxaliplatin and irinotecan resistance on colorectal cancers. Mol Med Rep. 2016;14:4893–4900.
14. Abella V, Scotece M, Conde J, GÃ³mez R, Lois A, Pino J, et al. The potential of lipocalin-2/NGAL as biomarker for inflammatory and metabolic diseases. Biomarkers 2015;20:565–71.
15. Wang Q, Li S, Tang X, Liang L, Wang F, Du H. Lipocalin 2 protects against escherichia coli infection by modulating neutrophil and macrophage function. Front Immunol. 2019;10:2594.
16. Borkham-Kamphorst E, Van de Leur E, Meurer SK, Buhl EM, Weiskirchen R. N-glycosylation of lipocalin 2 is not required for secretion or exosome targeting. Front Pharmacol. 2018;9:426.
17. Santiago-Sánchez GS, Pita-Grisanti V, Quiñones-Díaz B, Gumpper K, Cruz-Monserrate Z, Vivas-Mejía PE. Biological Functions and Therapeutic Potential of Lipocalin 2 in Cancer. Int J Mol Sci. 2020;21:4365.
18. Ong KL, Wu L, Januszewski AS, O'Connell RL, Xu A, Rye KA, et al. Relationships of adipocyte-fatty acid binding protein and lipocalin 2 with risk factors and chronic complications in type 2 diabetes and effects of fenofibrate: A fenofibrate Intervention and event lowering in diabetes sub-study. Diabetes Res Clin Pract. 2020;169:108450.
19. Miao Q, Ku AT, Nishino Y, Howard JM, Rao AS, Shaver TM, et al. Tcf3 promotes cell migration and wound repair through regulation of lipocalin 2. Nat Commun. 2014;5:4088 https://doi.org/10.1038/ncomms5088.
20. Viau A, El KK, Laouari D, Burtin M, Nguyen C, Mori K, et al. Lipocalin 2 is essential for chronic kidney disease progression in mice and humans. J Clin Investig. 2010;120:4065–76.
21. Yang J, Bielenberg DR, Rodig SJ, Doiron R, Clifton MC, Kung AL, et al. Lipocalin 2 promotes breast cancer progression. Proc Natl Acad Sci USA. 2009;106:3913–8.
22. Gomez-Chou SB, Swidnicka-Siergiejko AK, Badi N, Chavez-Tomar M, Lesinski GB, Bekaii-Saab T, et al. Lipocalin-2 promotes pancreatic ductal adenocarcinoma by regulating inflammation in the tumor microenvironment. Cancer Res. 2017;77:2647–60.
23. Tung MC, Hsieh SC, Yang SF, Cheng CW, Tsai RT, Wang SC, et al. Knockdown of lipocalin-2 suppresses the growth and invasion of prostate cancer cells. Prostate. 2013;73:1281–90.
24. Chi Y, Remsik J, Kiseliovas V, Derderian C, Sener U, Alghader M, et al. Cancer cells deploy lipocalin-2 to collect limiting iron in leptomeningeal metastasis. Science. 2020;369:276–82.
25. Sun Y, Yokoi K, Li H, Gao J, Hu L, Liu B, et al. NGAL expression is elevated in both colorectal adenoma-carcinoma sequence and cancer progression and enhances tumorigenesis in xenograft mouse models. Clin Cancer Res. 2011;17:4331–40.
26. Guo X, Li Q, Wang YF, Wang TY, Chen SJ, Tian ZW. Reduced lipocalin 2 expression contributes to vincristine resistance in human colon cancer cells. Recent Pat Anticancer Drug Discov. 2018;13:248–54.

27. Leung L, Radulovich N, Zhu CQ, Organ S, Bandarchi B, Pintilie M. et al. Lipocalin2 promotes invasion, tumorigenicity and gemcitabine resistance in pancreatic ductal adenocarcinoma. PLoS ONE. 2012;7:e46677.
28. Kim SL, Min IS, Park YR, Lee ST, Kim SW. Lipocalin 2 inversely regulates TRAIL sensitivity through p38 MAPK-mediated DR5 regulation in colorectal cancer. Int J Oncol. 2018;53:2789–99.
29. Huang Z, Zhang Y, Li H, Zhou Y, Zhang Q, Chen R, et al. Vitamin D promotes the cisplatin sensitivity of oral squamous cell carcinoma by inhibiting LCN2-modulated NF- B pathway activation through RPS3. Cell Death Dis. 2019;10:936–2177.
30. Arachiche A, Augereau O, Decossas M, Pertuiset C, Gontier E, Letellier T, et al. Localization of PTP-1B, SHP-2, and Src exclusively in rat brain mitochondria and functional consequences. J Biol Chem. 2008;283:24406–11.
31. Arias-Salgado EG, Lizano S, Sarkar S, Brugge JS, Ginsberg MH, Shattil SJ. Src kinase activation by direct interaction with the integrin beta cytoplasmic domain. Proc Natl Acad Sci USA. 2003;100:13298–302.
32. Rosenzweig SA. Acquired resistance to drugs targeting tyrosine kinases. Adv Cancer Res. 2018;138:71–98.
33. Zhang X, Chen Y, Hao L, Hou A, Chen X, Li Y, et al. Macrophages induce resistance to 5-fluorouracil chemotherapy in colorectal cancer through the release of putrescine. Cancer Lett. 2016;381:305–13.
34. Wang Z, Zhao X, Wang W, Liu Y, Li Y, Gao J, et al. ZBTB7 evokes 5-fluorouracil resistance in colorectal cancer through the NF B signaling pathway. Int. J. Oncol. 2018;53:2102–10.
35. Belli S, Esposito D, Servetto A, Pesapane A, Formisano L, Bianco R. c-Src and EGFR inhibition in molecular cancer therapy: what else can we improve? Cancers. 2020;12:1489.
36. Martínez-Pérez J, Lopez-Calderero I, Saez C, Benavent M, Limon ML, Gonzalez-Exposito R, et al. Prognostic relevance of Src activation in stage II-III colon cancer. Hum Pathol. 2017;67:119–25.
37. Griffiths GJ, Koh MY, Brunton VG, Cawthorne C, Reeves NA, Greaves M, et al. Expression of kinase-defective mutants of c-Src in human metastatic colon cancer cells decreases Bcl-xL and increases oxaliplatin- and Fas-induced apoptosis. J Biol Chem. 2004;279:46113–21.
38. Jin W. Regulation of Src family kinases during colorectal cancer development and its clinical implications. Cancers. 2020;12:1339.
39. Perez M, Lucena-Cacace A, MarÃn-GÃ³mez LM, Padillo-Ruiz J, Robles-Frias MJ, Saez C, et al. Dasatinib, a Src inhibitor, sensitizes liver metastatic colorectal carcinoma to oxaliplatin in tumors with high levels of phospho-Src. Oncotarget. 2016;7:33111–24.
40. Dunn EF, Iida M, Myers RA, Campbell DA, Hintz KA, Armstrong EA, et al. Dasatinib sensitizes KRAS mutant colorectal tumors to cetuximab. Oncogene. 2011;30:561–74.
41. Roskoski R Jr. Src protein-tyrosine kinase structure, mechanism, and small molecule inhibitors. Pharmacol Res. 2015;94:9–25.
42. Reinecke JB, Katafiasz D, Naslavsky N, Caplan S. Regulation of Src trafficking and activation by the endocytic regulatory proteins MICAL-L1 and EHD1. J Cell Sci. 2014;127:1684–98.
43. Xiao R, Xi XD, Chen Z, Chen SJ, Meng G. Structural framework of c-Src activation by integrin 3. Blood. 2013;121:700–6.
44. Desgrosellier JS, Barnes LA, Shields DJ, Huang M, Lau SK, Prevost N, et al. An integrin alpha(v)beta(3)-c-Src oncogenic unit promotes anchorage-independence and tumor progression. Nat Med. 2009;15:1163–9.
45. Brown R, Curry E, Magnani L, Wilhelm-Benartzi CS, Borley J. Poised epigenetic states and acquired drug resistance in cancer. Nat Rev Cancer. 2014;14:747–53.
46. Meka P, Jarjapu S, Nanchari SR, Vishwakarma SK, Edathara PM, Gorre M, et al. LCN2 promoter methylation status as novel predictive marker for microvessel density and aggressive tumor phenotype in breast cancer patients. Asian Pac J Cancer Prev. 2015;16:4965–9.
47. Conde J, Otero M, Scotece M, Abella V, López V, Pino J, et al. E74-like factor 3 and nuclear factor- B regulate lipocalin-2 expression in chondrocytes. J Physiol. 2016;594:6133–46.
48. Wu C, Qiu S, Lu L, Zou J, Li WF, Wang O, et al. RSPO2-LGR5 signaling has tumour-suppressive activity in colorectal cancer. Nat Commun. 2014;5:3149.
49. Chen T, Dai X, Dai J, Ding C, Zhang Z, Lin Z, et al. AFP promotes HCC progression by suppressing the HuR-mediated Fas/FADD apoptotic pathway. Cell Death Dis. 2020;11:822–03030.
50. Dong X, Liao W, Zhang L, Tu X, Hu J, Chen T, et al. RSPO2 suppresses colorectal cancer metastasis by counteracting the Wnt5a/Fzd7-driven noncanonical Wnt pathway. Cancer Lett. 2017;402:153–65.

ACKNOWLEDGEMENTS

This work was supported by National Natural Science Foundation of China (Grant Nos. 81972765 and 81772966) and Zhejiang Provincial Natural Science Foundation (No. LZ21H160007). The Superbiotek Inc. (Shanghai, China) provided CRC tissue microarray analysis. The authors also thank the Laboratory Animal Research Center in Wenzhou Medical University for technical assistance.

AUTHOR CONTRIBUTIONS

WZ designed, performed experiments, analyzed the data, and was a major contributor in writing the manuscript. RP and ML analyzed and interpreted the patient data. QZ, ZW, SG and HL partially contributed to the experiments presented in this manuscript. ZL and YQ contributed to the animal care and experiments. SC and LL provided technical assistance. WL provided assistance in manuscript writing. XL conceived the study, designed the experiments, and wrote and finalized the manuscript. All authors read and approved the final manuscript.

COMPETING INTERESTS

The authors declare no competing interests.

ADDITIONAL INFORMATION

Supplementary information The online version contains supplementary material available at https://doi.org/10.1038/s41388-021-02029-4.

Correspondence and requests for materials should be addressed to Xincheng Lu.

Reprints and permission information is available at http://www.nature.com/reprints

Publisher's note Springer Nature remains neutral with regard to jurisdictional claims in published maps and institutional affiliations.